NUMERICAL COMPUTATION OF THE FLOW WITH A SHOCK WAVE PASSING THROUGH A "STRONG EXPLOSION" CENTER*

WU XIONG-HUA(吴雄华) (*Computing Centre, Academia Sinica*)
HUANG DUN(黄 敦) (*Beijing University*)
ZHU YOU-LAN(朱幼兰) (*Computing Centre, Academia Sinica*)

1. Introduction

When a strong plane explosion wave impinges normally upon a rigid wall, a plane reflected wave forms. It propagates into the region disturbed by the explosion. This paper is a sequel to [2] and [4]. We use exact quasilinear equations of gasdynamics with Euler's coordinate and time and exact gasdynamic shock conditions. The problem was treated by many existing excellent methods. But we realized that without special treatment it is hardly possible to compute the propagation of the reflected wave until it reaches the explosion center, and it is even more difficult to calculate further propagation of the reflected shock. The difficulty is due to the fact that in the model of the so-called "point explosion", the gas temperature and the speed of propagation of the shock wave tend to infinity as the explosion center is approached. On the basis of analysis of the singular behavior of the solution and further development of the "singularity-separating method" we successfully overcome the above mentioned difficulty. In this paper the results of the flow behind the reflected shock are presented, describing how the reflected wave reaches and passes the explosion center. Further results of the flow field are obtained for all time until the reflected wave propagates to a distance about three times the distance from the wall to the explosion center. After the reflected wave interacts with the explosion center, one should treat carefully a curved trajectory with vanishing density as well as a new shock wave propagating towards the rigid wall. The new shock forms from the intersection of the characteristic lines of the same second family. Numerical results are satisfactory, which means that our singularity-separating method is efficient for solving this kind of problems with rather complex singularity.

2. Formulation of the Problem

Huang has presented the formulation of our problem of unsteady plane motion of a perfect gas in [2]. In that formulation the following system of equations of gasdynamics is used:

* Received December 7, 1982.

$$\begin{cases} \dfrac{\partial u}{\partial t}+u\dfrac{\partial u}{\partial x}+\dfrac{1}{\rho}\dfrac{\partial p}{\partial x}=0, \\ \dfrac{\partial \rho}{\partial t}+u\dfrac{\partial \rho}{\partial x}+\rho\dfrac{\partial u}{\partial x}=0, \\ \dfrac{\partial p}{\partial t}+u\dfrac{\partial p}{\partial x}+\gamma p\dfrac{\partial u}{\partial x}=0. \end{cases} \tag{1}$$

Suppose that at time $t=-t_1(t_1>0)$, a "strong" explosion at the plane $x=R_0$ appears. "Strong" explosion means that the initial energy and the pressure of the static gas in front of the explosion wave can be neglected when compared with the energy released per unit area E. The explosion wave AO (Fig. 1) moves towards the rigid wall $x=0$. At $t=0$ it meets the wall $x=0$, and ODB denotes the reflected wave. Thus there are three regions as shown in Fig. 1 on the x–t plane: region I (the region behind the strong plane explosion wave where there is a selfsimilar solution), region II (the unsteady gas flow behind the reflected wave which is neither isentropic nor selfsimilar) and region III ($\rho_0\neq 0$, $p=u=e=0$).

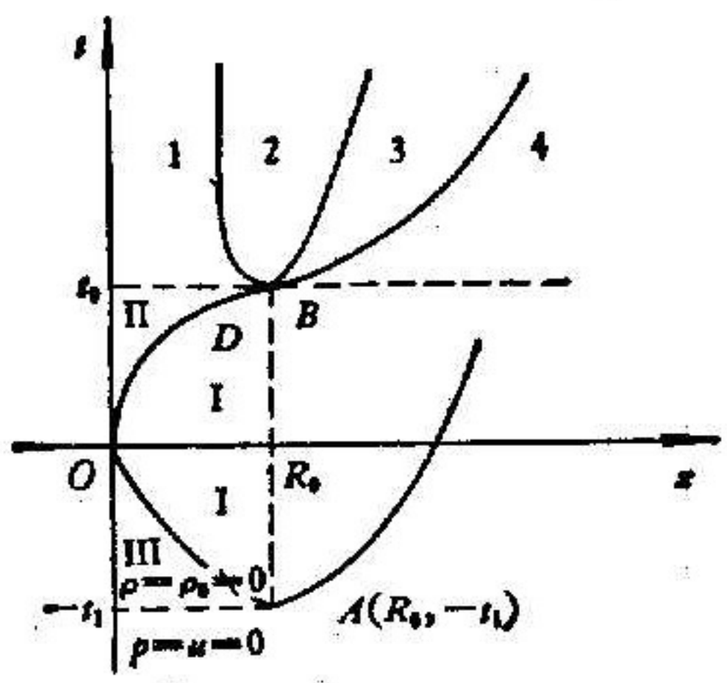

Fig. 1

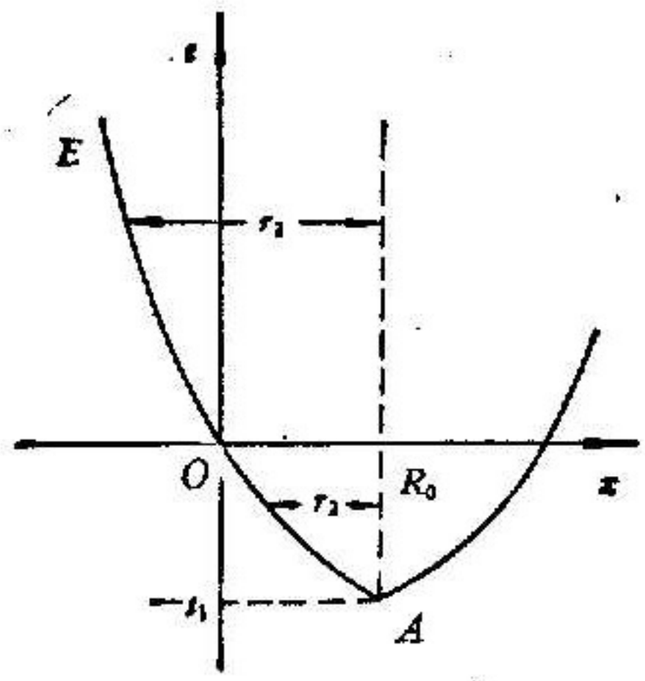

Fig. 2

The selfsimilar solution for region I is given in [2] and [3]: If there is no wall, the wave AO will propagate towards the left as shown by curve AOE in Fig. 2. According to [2], the distance r_2 between AOE and $x=R_0$ is given by

$$r_2=\left(\frac{E}{\rho_0}\right)^{1/3}(t+t_1)^{2/3},$$

then $R_0=\left(\dfrac{E}{\rho_0}\right)^{1/3}t_1^{2/3}$ and

$$\frac{dr_2}{dt}=V=\frac{2}{3}\frac{r_2}{t+t_1},$$

V being the speed of the explosion wave. Set $R_0=0.1$ m, $E=2734905.6$ J/m^2, $t_1=0.21718193\times 10^{-4}$s, $\rho_0=1.29$ kg/m^3 and the specific-heat ratio $\gamma=1.4$. The pressure behind the reflected shock at the origin of x–t diagram is just 800 atm. Since $p=u=e=0$ in region III, immediately behind the incident wave AOE the gas density $\bar{\rho}=6\rho_0$, the particle velocity $\bar{v}=V/1.2$ and the pressure $\bar{p}=\dfrac{1}{1.2}\rho_0V^2$. Denote $(R_0-x)/r_2$ by $R(x,\ t)$. It relates to a parameter $\tilde{V}$ by the relation[2]

$$R=(1.8\tilde{V})^{-2/3}(12.6\tilde{V}-6)^{2/9}(3-3.6\tilde{V})^{-5/2}, \tag{2}$$

then u, p, ρ in the region I can be expressed by

$$u=-\bar{\nu}(1.8R\sqrt{\nabla}), \tag{3}$$

$$\rho=\bar{\rho}(12.6\sqrt{\nabla}-6)^{5/2}(6-9\sqrt{\nabla})^{-10/3}(3-3.6\sqrt{\nabla})^{25/2}, \tag{4}$$

$$p=\bar{p}(1.8\sqrt{\nabla})^{2/3}(6-9\sqrt{\nabla})^{-7/3}(3-3.6\sqrt{\nabla})^{5/3}. \tag{5}$$

Wu has obtained in [4] satisfactory numerical solutions in region II using the singularity-separating method for this problem. Results were obtained when the distance of the reflected shock wave from the wall is less than or equal to 0.096 m. Further calculation, that is, to extend further the reflected shock towards the explosion center B, is difficult because of the singularity along $x=R_0$, for $t<t_0$. In this paper the singularity-separating method is developed to account for the singularity along $x=R_0$ and we have obtained the solution until the reflected shock reaches and then passes $B(x=R_0)$. The method consists of two parts as explained in the next section.

3. Numerical Methods

I. *A method which enables us to continue the computation until the reflected shock reaches the explosion center.*

We developed the singularity-separating method for the computation of the flow field in the case where the reflected wave from the wall reaches the explosion point. In [1] a method was devised to treat the interaction of discontinuities of shock or contact discontinuity type. In this method discontinuity lines are treated as unknown internal boundaries, so that there is no discontinuity of flow variables in each subregion; when one meets a centered rarefaction fan the multivalue point can be treated by transforming the independent variables. In this part we overcome the difficulty caused by singularity along $x=R_0$ by transforming the physical quantities, thereby we can easily obtain the numerical solution when the reflected wave OD reaches $B(x=R_0)$. We should mention that the results of this paper can be further improved.

Denote by $r=|0.1-x|$ the distance between a point in x–t plane from the line $x=R_0$. We use subscript 1 to denote the quantities in front of curve OB, and subscript 2 to denote quantities behind it. Then shock relations along OB are

$$\begin{aligned} p_2&=p_1(1+z)=p_1\Big[1+\frac{7}{6}(M^{*2}-1)\Big],\\ \rho_2&=\rho_1(2\gamma+(\gamma+1)z)/(2\gamma+(\gamma-1)z),\\ u_2&=u_1+zc_1/(\gamma\sqrt{1+(\gamma+1)z/(2\gamma)})=u_1+\frac{2}{\gamma+1}\Big(M^*-\frac{1}{M^*}\Big)c_1. \end{aligned} \tag{6}$$

Here, $z=(p_2-p_1)/p_1$ expresses the strength of the shock wave, M^*, the shock Mach number, and $c_1=\sqrt{\gamma p_1/\rho_1}$, the local sound speed.

From the definition of R and r we see that for small r, $r\sim R$, and further from (2) and (4) $\rho_1\sim(12.6\sqrt{\nabla}-6)^{5/2}\sim R^{5/2}\sim r^{5/2}$ when r tends to zero. When shock wave moves towards the explosion point, the shock Mach number M^* tends to 1 and the strength of the shock z tends to 0, thus

$$\rho_2\sim\rho_1\sim r^{5/2}. \tag{7}$$

$$c_2\sim c_1\sim\sqrt{\gamma p_1/\rho_1}\sim r^{-5/4}. \tag{8}$$

From (3) we know that u_1 tends to zero, and

$$V=u_1+\left(1+\frac{\gamma+1}{2\gamma}z\right)^{1/2}\cdot c_1\sim c_1\sim r^{-5/4}. \tag{9}$$

In his lecture given in Beijing University, Huang Dun presented estimates of flow variables in region II for small r based on Whitham's "characteristic rule":

$$dp_2+\rho_2 c_2 du_2=0. \tag{10}$$

Differentiation of the first and third of (6) while neglecting dp_1, which is small, gives

$$dp_2=p_1\cdot\frac{7}{3}M^*dM^*,$$

$$du_2=\frac{2}{\gamma+1}\left(M^*-\frac{1}{M^*}\right)\left(-\frac{1}{2}\right)\frac{c_1}{\rho_1}d\rho_1+\frac{2c_1}{\gamma+1}\left(1+\frac{1}{M^{*2}}\right)dM^*+du_1.$$

From (7) one has

$$\frac{d\rho_1}{\rho_1}=2.5\frac{dr}{r}.$$

Substituting the above relations into (10), a relation between M^* and r is obtained:

$$\left\{\sqrt{\frac{6+(M^{*2}-1)}{6+7(M^{*2}-1)}}+\frac{1}{2}\left(1+\frac{1}{M^{*2}}\right)\right\}dM^*=\frac{M^{*2}-1}{4M^*}2.5\frac{dr}{r}-\frac{3}{5c_1}du_1.$$

Here, du_1 is much smaller than other terms and so can be omitted. Let the quantities in the external brackets on the left side be $2F(M^*)$, then we have

$$\lim_{M^*\to 1}F(M^*)=1,$$

$$\int F(M^*)\frac{d(M^{*2}-1)}{M^{*2}-1}=\int\frac{5}{8}\frac{dr}{r},$$

$$\frac{M^{*2}-1}{M^*}\sim r^{0.625}. \tag{11}$$

Substituting (11) into shock relations we obtain the following estimates

$$u_2=u_1+\frac{2}{\gamma+1}\left(\frac{M^{*2}-1}{M^*}\right)c_1\sim r^{0.625}c_1\sim r^{-0.625}. \tag{11}'$$

On the basis of (7), (8), (9), (11)′, in region II we introduce the following new variables:

$$u=r^{-0.625}v,\quad \rho=r^{2.5}w,\quad p=p,$$
$$c=r^{-1.25}\hat{c},\quad V=r^{-1.25}\hat{V}.$$

Then the system of equations (1) is transformed to

$$\begin{cases}\dfrac{\partial v}{\partial t}+r^{-0.625}v\dfrac{\partial v}{\partial x}+r^{-1.875}\dfrac{1}{w}\dfrac{\partial p}{\partial x}=-0.625r^{-1.625}v^2,\\ \dfrac{\partial w}{\partial t}+r^{-0.625}v\dfrac{\partial w}{\partial x}+r^{-0.625}w\dfrac{\partial v}{\partial x}=1.875\,r^{-1.625}vw,\\ \dfrac{\partial p}{\partial t}+r^{-0.625}v\dfrac{\partial p}{\partial x}+r^{-0.625}\gamma p\dfrac{\partial v}{\partial x}=-0.625r^{-1.625}\gamma pv.\end{cases}$$

Adopting this system of equations makes the calculation possible for the case $r\approx 0$ (Thus we say that we have further developed the singularity separating method in this paper). To transform the above system of equations into characteristic form, we multiply the matrix

$$\bar{G}=\begin{bmatrix} w\hat{c} & 0 & r^{-0.625} \\ 0 & \gamma p & -w \\ -w\hat{c} & 0 & r^{-0.625} \end{bmatrix}$$

from the left side, and obtain

$$\bar{G}\frac{\partial \bar{U}}{\partial t}+\bar{\Lambda}\bar{G}\frac{\partial \bar{U}}{\partial x}=\bar{F}, \tag{12}$$

where $\bar{\lambda}_1=r^{-0.625}v+r^{-1.25}\hat{c}$, $\bar{\lambda}_2=r^{-0.625}v$, $\bar{\lambda}_3=r^{-0.625}v-r^{-1.25}\hat{c}$,

$$\bar{U}=\begin{bmatrix} v \\ w \\ p \end{bmatrix},\quad \bar{\Lambda}=\begin{bmatrix} \lambda_1 & 0 & 0 \\ 0 & \lambda_2 & 0 \\ 0 & 0 & \lambda_3 \end{bmatrix},\quad \bar{F}=-0.625r^{-1.625}v\begin{bmatrix} w\hat{c}v+r^{-0.625}\gamma p \\ -4w\gamma p \\ -w\hat{c}v+r^{-0.625}\gamma p \end{bmatrix}.$$

We can transform the subregion whose boundaries are $x=0$ and $x_1(t)$ into a strip $0\leqslant\xi\leqslant 1$ in the ξ–t plane by using the transformation $t=t$, $\xi=x/x_1(t)$. Here the unknown function $x_1(t)$ describes the curve OB in Fig. 1. Then the system of equations (12) is transformed into

$$G_n\frac{\partial U}{\partial t}+\lambda_n G_n\frac{\partial U}{\partial \xi}=f_n,\quad n=1,\ 2,\ 3, \tag{13}$$

where

$$U(\xi,\ t)=\bar{U}(x,\ t)=\begin{bmatrix} v \\ w \\ p \end{bmatrix},$$

G_n is the n–th row of

$$G=\begin{bmatrix} w\hat{c} & 0 & (0.1-x_1(t)\xi)^{-0.625} \\ 0 & \gamma p & -w \\ -w\hat{c} & 0 & (0.1-x_1(t)\xi)^{-0.625} \end{bmatrix}$$

while f_n is the n–th component of

$$F=-0.625(0.1-x_1(t)\xi)^{-1.625}v\begin{bmatrix} w\hat{c}v+(0.1-x_1(t)\xi)^{-0.625}\gamma p \\ -4w\gamma p \\ -w\hat{c}v+(0.1-x_1(t)\xi)^{-0.625}\gamma p \end{bmatrix}$$

and $\lambda_n=\dfrac{\partial \xi}{\partial x}\bar{\lambda}_n+\dfrac{\partial \xi}{\partial t}=\dfrac{1}{x_1(t)}(\bar{\lambda}_n-\xi x_1'(t))$.

For simplicity we omit the subscript n of λ_n, G_n and f_n in the difference equations. Denote $\sigma=\lambda\Delta t/\Delta\xi$, $u_m^k=u(\xi_m,\ t_k)$, and use similar notations for other quantities. [1] gives an explicit-implicit-mixed scheme, which is unconditionally stable. We compute quantities in region II using this scheme.

If $|\sigma|\leqslant 1$ we take the following two-step explicit scheme. At the auxiliary level the approximation is

$$G_m^k U_m^{k+\frac{1}{2}}=(1\mp\sigma_m^k/2)G_m^k U_m^k\pm(\sigma_m^k/2)G_m^k U_{m\mp1}^k+\Delta t f_m^k/2,$$

where we take the upper sign if $\sigma>0$ and the lower sign if $\sigma<0$. At the regular level the formula is

$$\frac{1}{2}((1-B_m)(G_{m+1}^{k+\frac{1}{2}}+G_m^{k+\frac{1}{2}})+B_m(G_m^{k+\frac{1}{2}}+G_{m-1}^{k+\frac{1}{2}}))U_m^{k+1}=(1-B_m)S_m^1+B_m S_m^2.$$

Here

$$S_m^1=(G_{m+1}^{k+\frac{1}{2}}+G_m^{k+\frac{1}{2}})U_{m+1}^k/2-((\sigma_{m+1}^{k+\frac{1}{2}}+\sigma_m^{k+\frac{1}{2}})/2+1)(G_{m+1}^{k+\frac{1}{2}}+G_m^{k+\frac{1}{2}})$$
$$\times(U_{m+1}^{k+\frac{1}{2}}-U_m^{k+\frac{1}{2}})/2+\Delta t(f_{m+1}^{k+\frac{1}{2}}+f_m^{k+\frac{1}{2}})/2;$$

$$S_m^2=(G_m^{k+\frac{1}{2}}+G_{m-1}^{k+\frac{1}{2}})U_{m-1}^k/2-((\sigma_m^{k+\frac{1}{2}}+\sigma_{m-1}^{k+\frac{1}{2}}/2-1)(G_m^{k+\frac{1}{2}}+G_{m-1}^{k+\frac{1}{2}})$$
$$\times(U_m^{k+\frac{1}{2}}-U_{m-1}^{k+\frac{1}{2}})/2+\Delta t(f_m^{k+\frac{1}{2}}+f_{m-1}^{k+\frac{1}{2}})/2;$$

$$B_m=\begin{cases} m/M_1 & & 0\leqslant m<M_1,\\ 0 & \lambda>0 & \\ 1 & \lambda<0 & M_1\leqslant m\leqslant M_2,\\ (m-M_2)/(M-M_2) & & M_2<m\leqslant M; \end{cases}$$

$$M_1=\begin{cases} 0 & \lambda>0 \text{ on } \xi=0,\\ \min\left\{E\left(\frac{\xi_1}{\Delta\xi}\right),\ M-1\right\} & \lambda\leqslant 0 \text{ on } \xi=0; \end{cases}$$

$[0,\ \xi_1]$ is the maximum interval among the intervals on which λ is nonpositive and whose left end is the point $\xi=0$;

$$M_2=\begin{cases} \max\left\{M-E\left(\frac{1-\xi_2}{\Delta\xi}\right),\ 1\right\} & \lambda\geqslant 0 \text{ on } \xi=1,\\ M & \lambda<0 \text{ on } \xi=1; \end{cases}$$

$[\xi_2,\ 1]$ is the maximum interval among the intervals on which λ is nonnegative and whose right end is the point $\xi=1$; M is the number of mesh points; and $E(x)$ is the integral part of x.

If $|\sigma|>1$, we take the following implicit scheme. At the auxiliary level the formula is

$$(1+(\sigma_{m+1}^k+\sigma_m^k)/2)(G_{m+1}^k+G_m^k)U_{m+1}^{k+\frac{1}{2}}+(1-(\sigma_{m+1}^k+\sigma_m^k)/2)(G_{m+1}^k+G_m^k)U_m^{k+\frac{1}{2}}$$
$$=(G_{m+1}^k+G_m^k)(U_{m+1}^k+U_m^k)+\Delta t(f_{m+1}^k+f_m^k).$$

At the regular level the formula is

$$(1+(\sigma_{m+1}^{k+\frac{1}{2}}+\sigma_m^{k+\frac{1}{2}})/2)(G_{m+1}^{k+\frac{1}{2}}+G_m^{k+\frac{1}{2}})U_m^{k+1}$$
$$+(1-(\sigma_{m+1}^{k+\frac{1}{2}}+\sigma_m^{k+\frac{1}{2}})/2)(G_{m+1}^{k+\frac{1}{2}}+G_m^{k+\frac{1}{2}})U_m^{k+1}$$
$$=(G_{m+1}^{k+\frac{1}{2}}+G_m^{k+\frac{1}{2}})(U_{m+1}^k+U_m^k)-\frac{1}{2}(\sigma_{m+1}^{k+\frac{1}{2}}+\sigma_m^{k+\frac{1}{2}})$$
$$\times(G_{m+1}^{k+\frac{1}{2}}+G_m^{k+\frac{1}{2}})(U_{m+1}^k-U_m^k)+2\Delta t(f_{m+1}^{k+\frac{1}{2}}+f_m^{k+\frac{1}{2}}).$$

This scheme is of second order accuracy. Its stability follows from the discussion in [1].

For each differential equation, difference equations can be obtained by using this scheme. Finally we have the following systems of equations:

$$\begin{cases} A_1^{(m)}U_{m+1}+A_2^{(m)}U_m=A_3^{(m)},\\ B_1^{(m)}U_{m+1}+B_2^{(m)}U_m=B_3^{(m)},\\ D_1^{(m)}U_{m+1}+D_2^{(m)}U_m=D_3^{(m)}, \quad m=0,\ 1,\ \cdots,\ M-1. \end{cases} \tag{14}$$

Eq. (14) can be solved by the double-sweep method. First we eliminate $U_1, \cdots, U_{M-1}$ from (14) and obtain the system of equations with U_0 and U_M:

$$\begin{cases} A_1U_M+A_2U_0=A_3, \\ B_1U_M+B_2U_0=B_3, \\ D_1U_M+D_2U_0=D_3. \end{cases} \tag{15}$$

In view of the boundary condition $v_0=0$ and eliminating w_0 and p_0 from (15), we obtain the equation

$$Av_M+Bw_M+Dp_M=F. \tag{16}$$

The quantities in front of the shock wave can be evaluated by the given analytic expressions (2)—(5). By using shock relations (6), we can obtain a nonlinear equation $f(z)=0$ from (16). Solving it, we obtain the strength of the shock z. Quantities u_M, ρ_M, p_M and the speed of the shock V can be easily obtained by using z. Then we can also calculate the quantities at the interior points in terms of the quantities on the boundary $x_1(t)$.

If the location of the shock wave is apart from the explosion point at $x=0.1$ we can compute the flow field in region II by the singularity-separating method used in [4]. In this case the location of the shock wave can be determined by using the following scheme with second order accuracy:

$$X^{k+\frac{1}{2}}=X^k+V^k\Delta t/2,$$

$$X^{k+1}=X^k+V^{k+\frac{1}{2}}\Delta t.$$

If the location of the shock wave is very near the explosion point B, we can obtain numerical solution by solving difference equations approximating (13). To calculate the location of the shock wave we make use of

$$\frac{dx}{dt}=V=(0.1-x)^{-1.25}\bar{V},$$

and thus

$$(0.1-x)^{1.25}dx=\bar{V}dt,$$

$$\int_{x^k}^{x^{k+1}}(0.1-x)^{1.25}\,dx=\int_t^{t+\Delta t}\bar{V}dt,$$

$$-\frac{1}{2.25}((0.1-X^{k+1})^{2.25}-(0.1-X^k)^{2.25})=\bar{V}^{k+\frac{1}{2}}\Delta t,$$

$$(0.1-X^{k+1})^{2.25}=(0.1-X^k)^{2.25}-2.25\Delta t\bar{V}^{k+\frac{1}{2}}.$$

In our computation we use the following scheme:

$$X^{k+\frac{1}{2}}=0.1-((0.1-X^k)^{2.25}-1.125\Delta t\bar{V}^k)^{4/9},$$

$$X^{k+1}=0.1-((0.1-X^k)^{2.25}-2.25\Delta t\bar{V}^{k+\frac{1}{2}})^{4/9}.$$

At $t=1.9925\times10^{-5}$, $x_1(t)$ is very close to but less than 0.1, then we change the time increment by setting $\Delta t=(0.1-X^k)^{2.25}/(2.25V^k)$. Finally we have the coordinates of B as $(0.1,\ 1.9938\times10^{-5})$. Although the above derivation is long, it enables us to overcome the difficulty caused by high temperature singularity and makes it possible to calculate the reflected shock wave till it reaches the explosion center B.

II. *The computation of flow field after the passage of the reflected wave through the explosion center.*

There remains difficulty if we want to compute further. Now we will describe the method for the computation of the flow field in the upper region of Fig. 1. By analysis of the flow we conclude that we should treat first of all the reflected wave with

increasing strength, as well as a singular-trajectory, along which the density is zero while the velocity and the pressure are continuous. Furthermore we should treat an additional left-facing shock wave as shown in the upper part of Fig. 1, i. e., for $t>t_0=1.9938\times10^{-5}$. The formation of this wave can be understood if we examine (8) and (11). One can see that the second family of characteristics starting from the curve OB intersects each other near B, which means formation of a new shock wave. We will explain how to calculate these three difficult unknown lines as well as the quantities in subregions 1, 2, 3 of the upper part of Fig. 1. We use still the singularity-separating method to avoid smearing of discontinuity lines. The quantities in subregion 4 can be computed by using (3), (4) and (5). Difficulty lies first in initiating the calculation of the three unknown lines, which we shall describe below. To calculate the flow variables between these lines we can transform the subregion whose boundaries are $x_i(t)$ and $x_{i+1}(t)$ into a strip $0\leqslant\xi\leqslant1$ on the ξ-t plane by using the transformation $t=t$, $\xi=(x-x_i(t))/(x_{i+1}(t)-x_i(t))$. We denote by $x_0(t)=0$ the location of the rigid wall, $x_1(t)$ the location of the left-facing shock wave at time t, $x_2(t)$ the location of the singular-trajectory and $x_3(t)$ the location of the right-facing shock wave——the reflected wave. Meanwhile we transform the system of equations (1) into the characteristic form:

$$G_n\frac{\partial U}{\partial t}+\lambda_nG_n\frac{\partial U}{\partial\xi}=0,\quad n=1,\ 2,\ 3.$$

Here

$$\lambda_1=(u+c-x_i'(t)-\xi(x_{i+1}'(t)-x_i'(t)))/(x_{i+1}(t)-x_i(t)),$$
$$\lambda_2=(u-x_i'(t)-\xi(x_{i+1}'(t)-x_i'(t)))/(x_{i+1}(t)-x_i(t)),$$
$$\lambda_3=(u-c-x_i'(t)-\xi(x_{i+1}'(t)-x_i'(t)))/(x_{i+1}(t)-x_i(t)),$$

G_n is the n-th row of the matrix

$$\begin{bmatrix}\rho c, & 0, & 1\\ 0, & \gamma p, & -\rho\\ -\rho c, & 0, & 1\end{bmatrix}\quad\text{and}\quad U=\begin{bmatrix}u\\ \rho\\ p\end{bmatrix}.$$

By aid of the above scheme a system of difference equations in the form (14) valid for each of the three subregions can be obtained. We eliminate $U_1,\ \cdots,\ U_{M-1}$ and obtain the system of equations with U_0 and U_M in the form (15) in each subregion. The quantities on the boundaries can be found by solving the system of nonlinear equations (15) for three subregions with appropriate boundary conditions. After these we can compute the quantities at the interior points in various subregions. The double-sweep method used is explained in [1].

Now we concentrate our attention on the initiation of computation for boundaries of subregions from 1 to 4. We have explained how to calculate flow quantities in region II up to the dotted line in Fig. 1. They are the initial value for subregions. The difficulty is that according to (7) and (11)′ the gas density ρ tends to zero and the particle velocity u_3 tends to infinite as reflected shock tends to $x=R_0$. Here we introduce the following approximation: The quantities at point B in subregion 1 can be obtained by using an extrapolation based on neighbouring points. The quantities near point B in subregion 4 can be obtained again by Whitham's characteristic rule, which gives $t_0=1.9938\times10^{-5}$ for $x=0.101$, by using (3), (4), (5) we can obtain u,

ρ, p. We regard these values as the initial values for subregion 4.

In a lecture delivered at Beijing University Huang Dun presented an analytical formula for the relation between the distance r and the shock Mach number M^* in the region near point B, on the basis of (10) and some physical reasoning, the details of which should be published elsewhere. He gives $M^*=1.0380$ at $x=0.101$. Then the strength of the right-facing shock wave $z_r=\frac{7}{6}(M^{*2}-1)=0.09035$. The initial strength of the newly formed shock wave which propagates towards the rigid wall (we shall call it the left-facing wave) is of course zero. By using the shock relations (6) we can thus obtain the quantities in the vicinity of the left end in subregion 2 and the right end in subregion 3: $u_{2,0}$, $\rho_{2,0}$, $p_{2,0}$, $u_{3,M}$, $\rho_{3,M}$, $p_{3,M}$. Here M is the total number of mesh points in each subregion. On the singular trajectory, $\rho=0$, u and p are continuous we take the approximation

$$u_{2,M}=u_{3,0}=\frac{1}{2}(u_{2,0}+u_{3,M}),$$

$$p_{2,M}=p_{3,0}=\frac{1}{2}(p_{2,0}+p_{3,M}),$$

$$\rho_{2,M}=\rho_{3,0}=5\times10^{-6} \quad \text{instead of zero.}$$

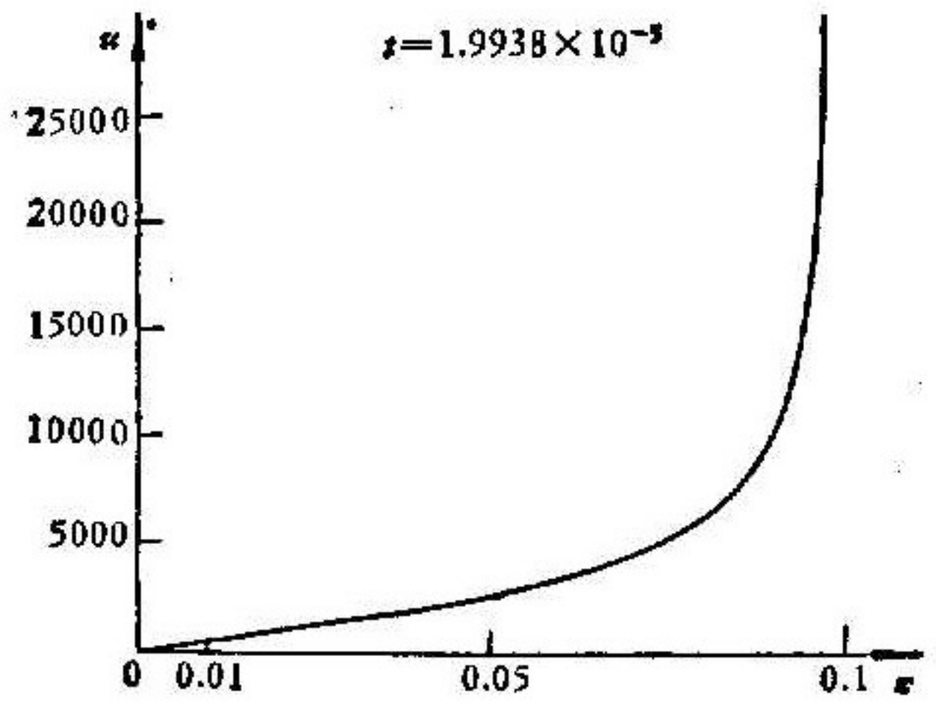

Fig. 3a

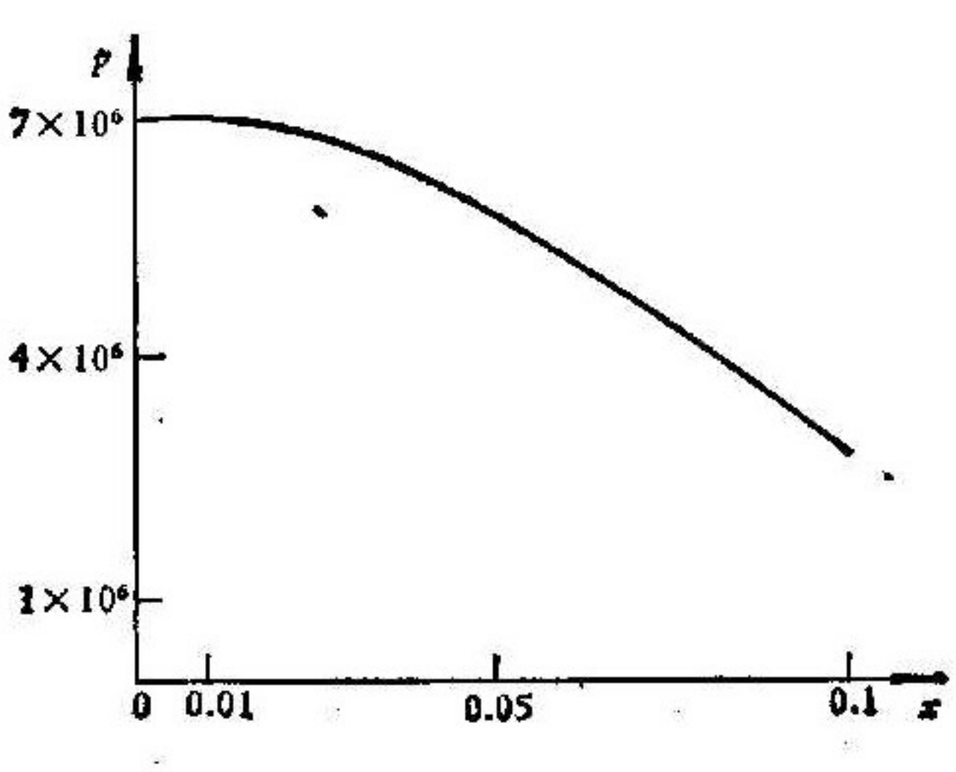

Fig. 3b

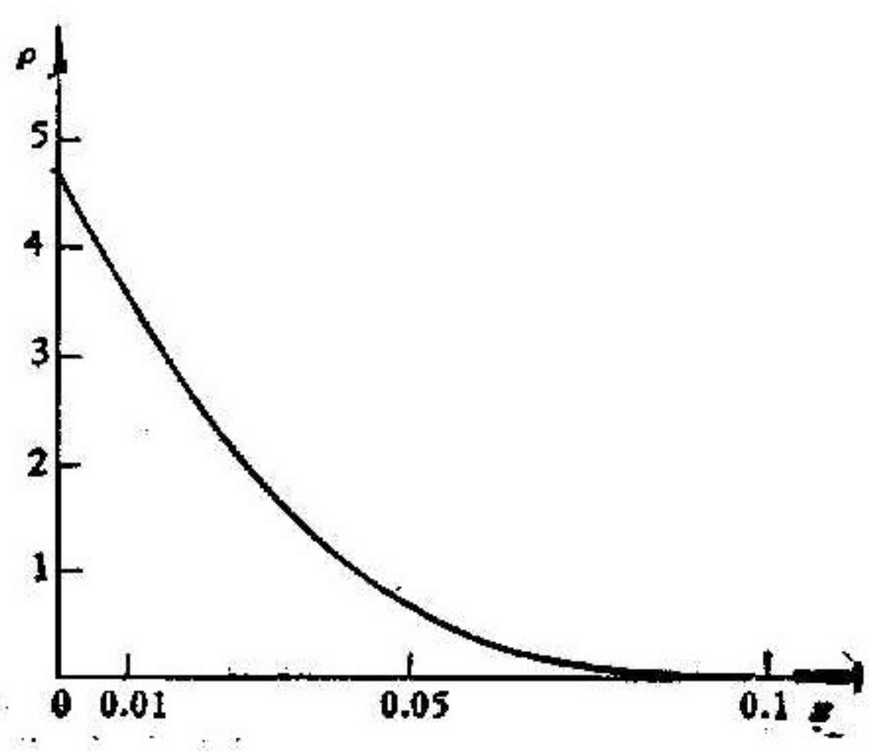

Fig. 3c

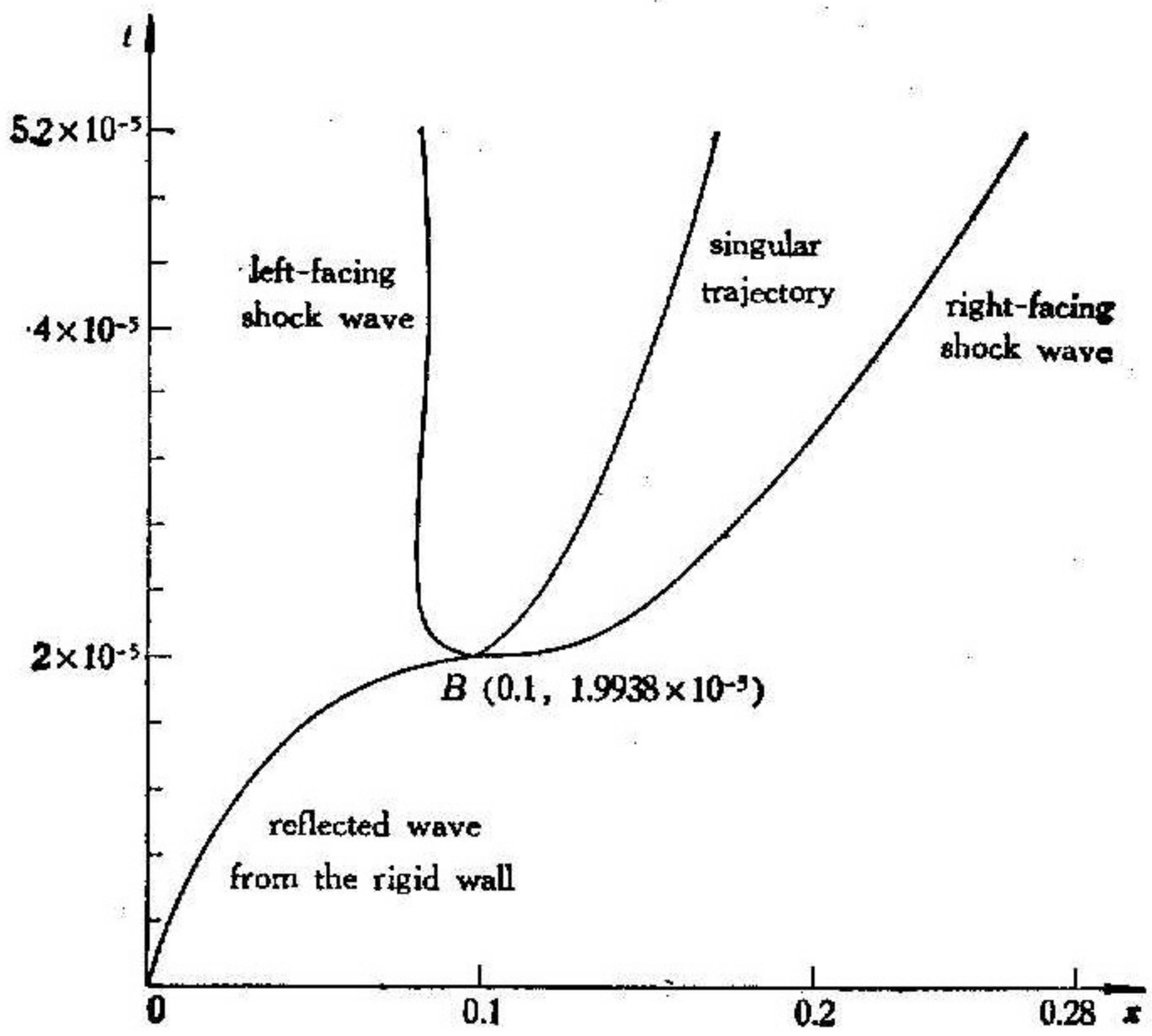

Fig. 4

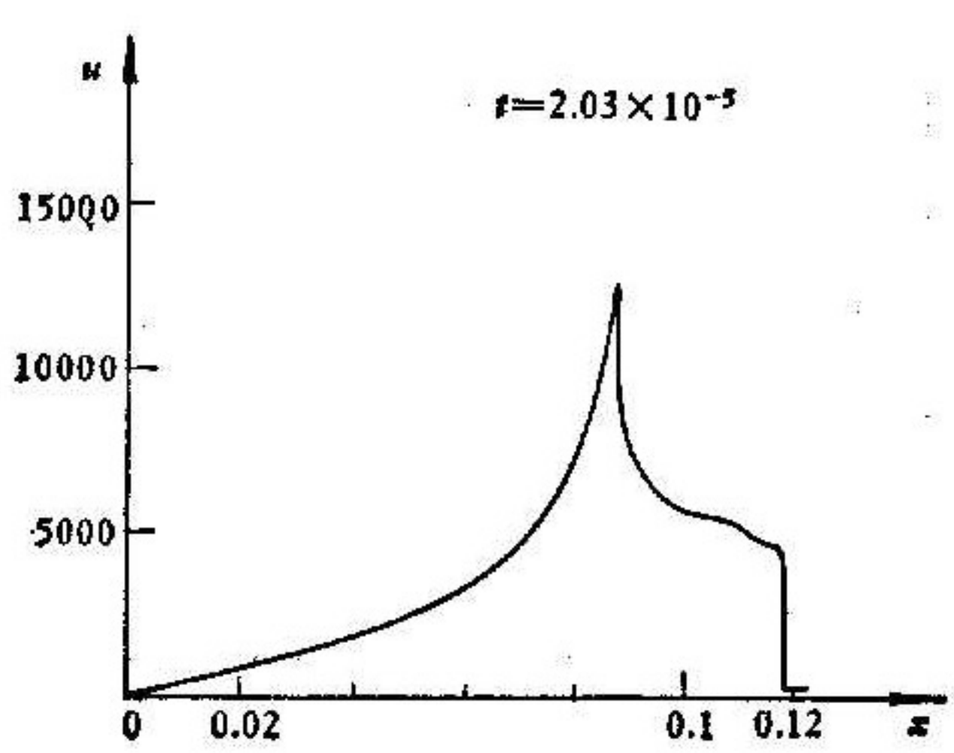

Fig. 5a

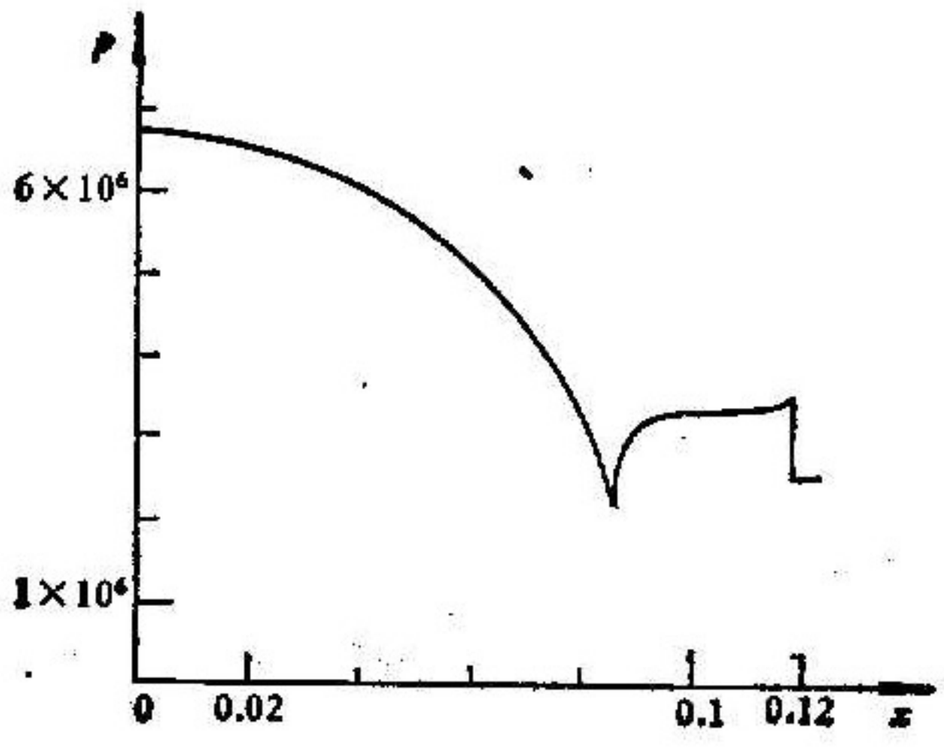

Fig. 5b

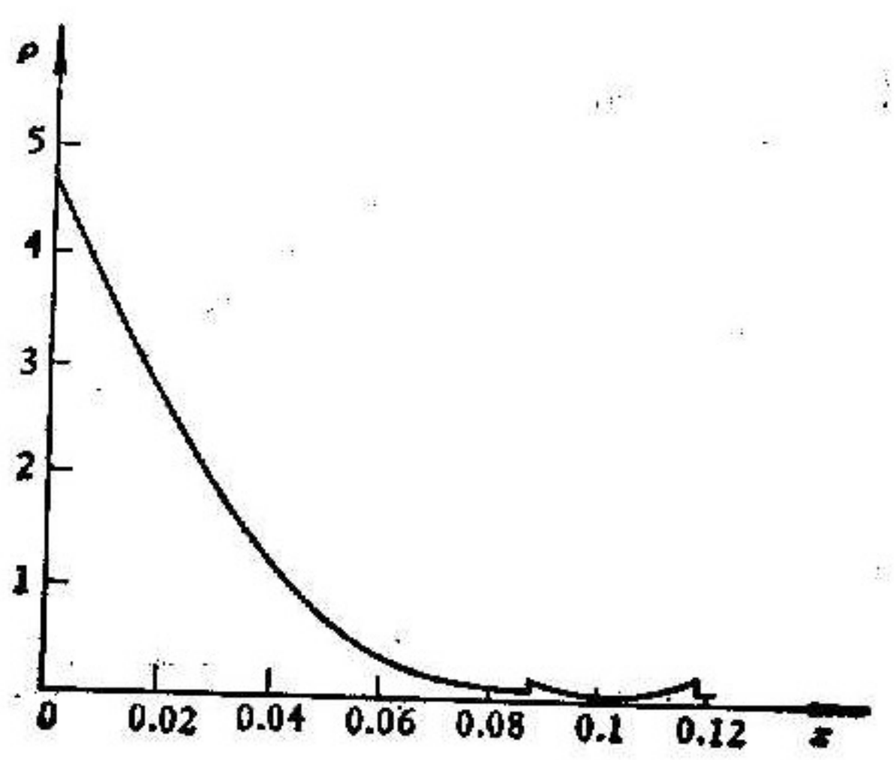

Fig. 5c

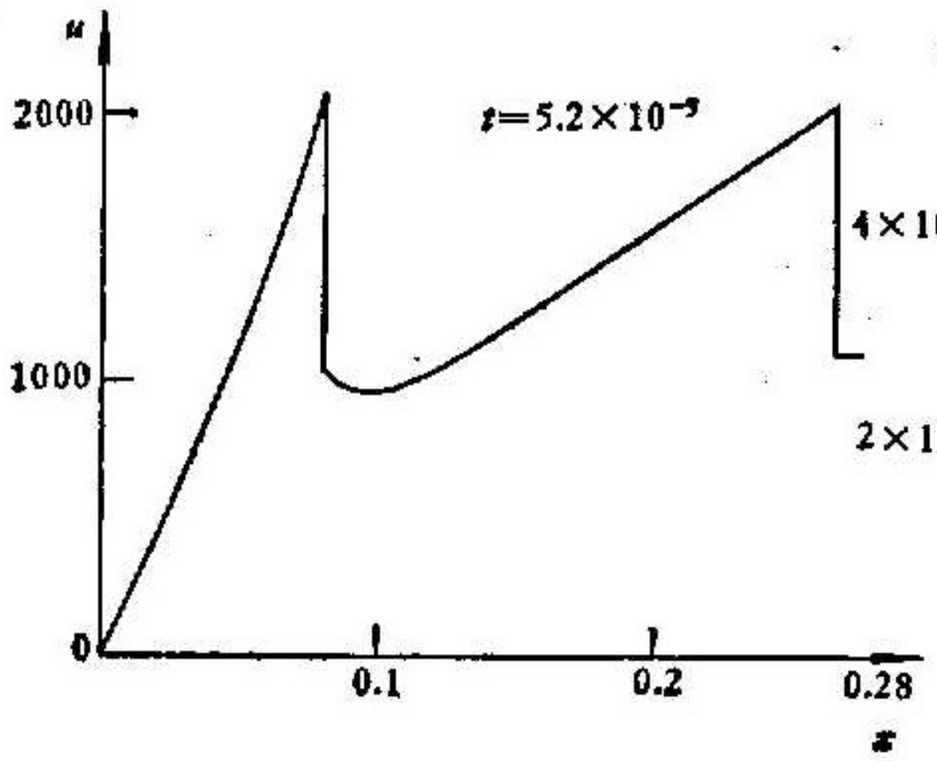

Fig. 6a

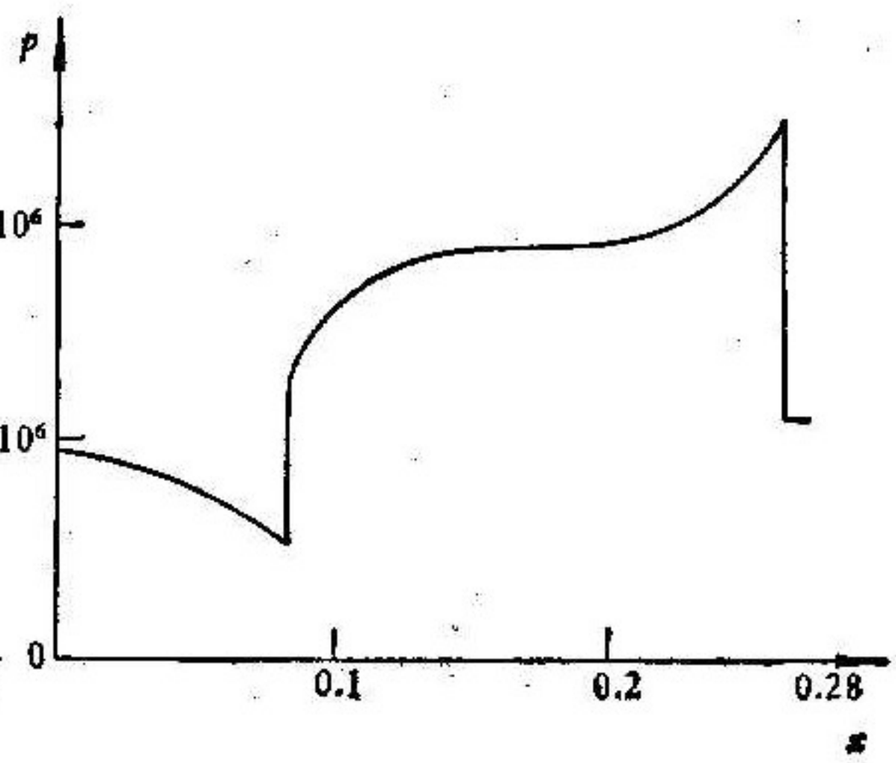

Fig. 6b

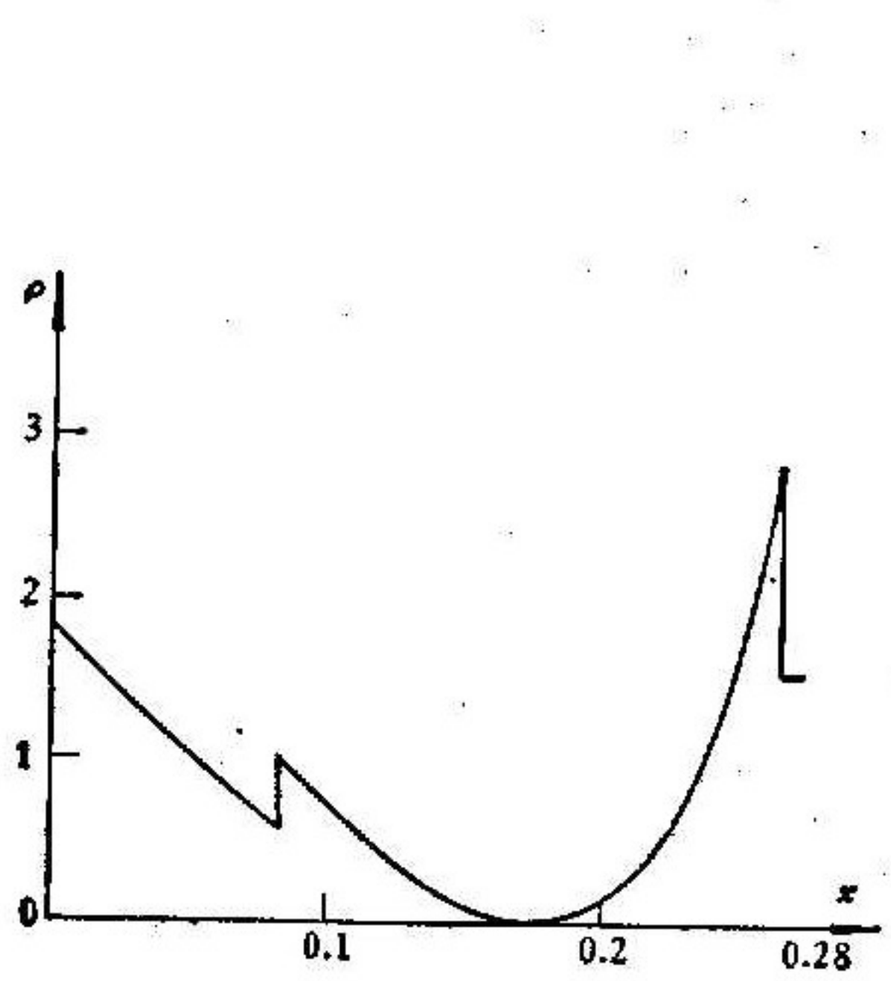

Fig. 6c

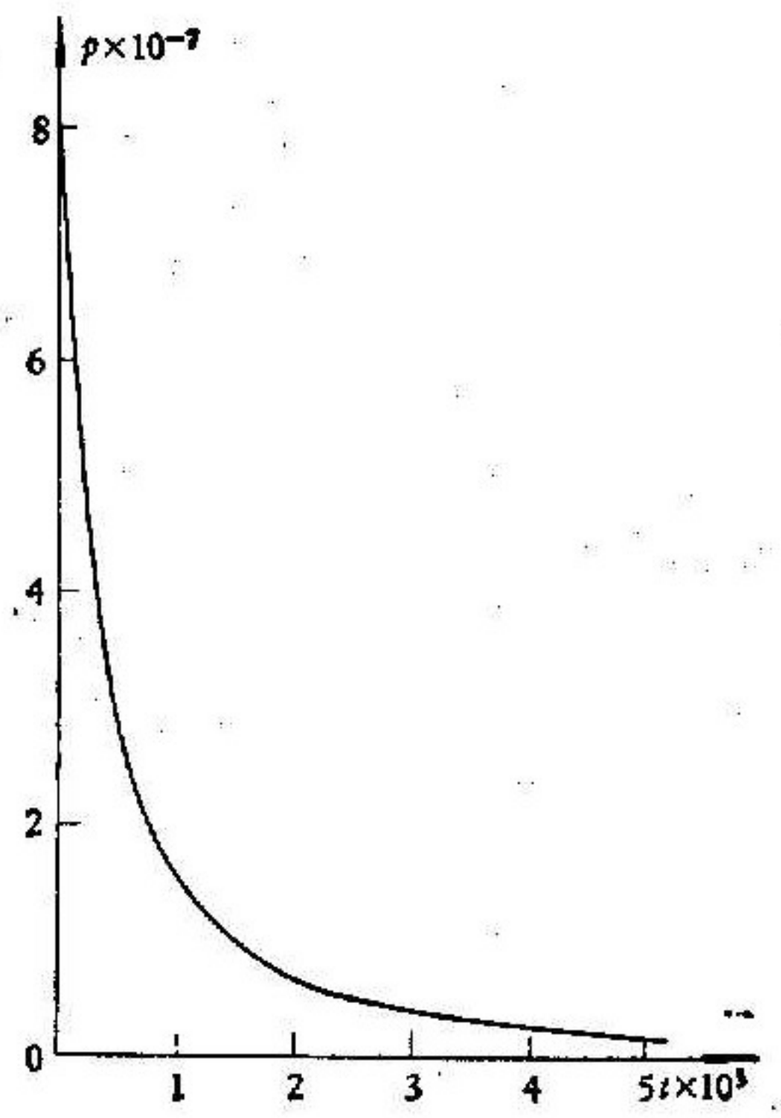

Fig. 7

Linear interpolation in subregions 2 and 3 respectively gives the initial values for these subregions. Thus we have explained how to treat the singularities near point B and how to obtain initial values for $t=t_0$.

4. Numerical Results

By using the singularity-separating method developed in this paper, we have obtained the distributions of u, p, ρ shown in Figs. 3a, 3b and 3c at time $t_0=1.9938\times10^{-5}$ (at this moment, the reflected shock wave reaches point B). The locations of the discontinuities in the whole flow field are described in Fig. 4. To evaluate the flow for $t>t_0$ we take $\Delta t=2\times10^{-8}$ and 40 mesh points in each subregion in the

computation. Typical results are shown by figures. Figs. 5a, b, c give for $t=t_0+20\Delta t=2.03\times10^{-5}$ the distributions of u, p, ρ. Figs. 6a, b, c describe for $t=t_0+1600\Delta t=5.2\times10^{-5}$ the distributions of u, p, ρ. The variation of pressure on the rigid wall is shown in Fig. 7.

From our numerical results we can make the following comments:

1) For $t>t_0$ the velocities, pressures and densities near the shock wave, especially near the left-facing shock change rapidly with x. If we use a method with artificial viscosity, the shock waves would be seriously smeared and the accuracy of computation would be poor. The singularity-separating method may evaluate these rapid changes very well.

2) The strengths of both the right-facing shock wave and the left-facing one $\left(\frac{p_2-p_1}{p_1}\right)$ increase slowly. They are about 1 for a certain long period.

3) The gas velocities in subregions 2 and 3 are very large when the reflected shock wave is located near point B, but they decreases soon. The accuracy of our results is high although some approximate treatment of velocity near point B is used. This is guaranteed by the stability of the scheme used.

4) In the computation we use $\rho\approx10^{-5}$ instead of vanishingly small quantities near the singular trajectory starting from point B. This approximate treatment will lead to some errors. But these errors will not increase owing also to the stability of our scheme. The density on the singular-trajectory is zero, and the sound speed C is infinity. This makes usual explicit schemes inapplicable for our problem in view of the Courant condition.

To sum up, we have presented in this paper satisfactory numerical results and a clear physical picture for this problem by using the singularity-separating method and its further development and making some approximate treatments near the singular point B of Fig. 1 based on analysis of the character of singularity (the analysis will be published elsewhere). Although the approximate treatments mentioned above can be further improved, our results are much more accurate than what could be obtained by any other of the existing methods, especially of shock-capturing type, since shocks and trajectory with zero density are treated separately and accurately.

References

[1] Zhu You-lan, Zhong Xi-chang, Chen Bing-mu, Zhang Zuo-min, Difference methods for initial boundary value problems and flow around bodies, Science Press, Beijing, China, 1980.

[2] Huang Dun, Normal reflection of a plane strong explosion wave, "Explosion and shock waves", 1981, Vol. 1. (in Chinese) See also Lecture Notes in Physics, Vol. 141, 218—223, Springer Verlag, 1981.

[3] L. I. Sedov, Similarity and dimensional methods in mechanics, 1957. (in Russian)

[4] Wu Xiong-hua, The application of the singularity-separating method to the computation of unsteady shock, *Journal of Numerical Methods and Computer Applications*, 1982, Vol. 3, No. 3. (in Chinese)